*First publ in:*
*Quantum mesoscopic phenomena and mesoscopic devices in microelectronics [Proceedings of the NATO Advanced Study Institute on Quantum Mesoscopic Phenomena and Mesoscopic Devices in Microelectronics, Ankara, Turkey, 13 - 25 June 1999] / ed. by Igor O. Kulik. 2000. Pp. 27-34*

# Chapter 2

# CONDUCTANCE CHANNELS OF GOLD ATOMIC-SIZE CONTACTS

E. Scheer
*Physikalisches Institut, Universität Karlsruhe*
*D-76128 Karlsruhe, Germany*

W. Belzig
*Department of Applied Physics & DIMES, Delft University of Technology*
*Lorentzweg 1, NL-2628 CJ Delft, The Netherlands*

M. H. Devoret, D. Esteve and C. Urbina
*Service de Physique de l'Etat Condensé Commissariat à l'Energie Atomique*
*Saclay, F-91191 Gif-sur-Yvette Cedex, France*

## 1. INTRODUCTION

Since the development of the scanning tunneling microscope (STM) [1] it is not only possible to see, but also to manipulate and to measure the transport properties of individual atoms on surfaces [2]. By energy dependent measurements of the differential conductance a certain chemical information can be achieved [3]. The challenging aim of building up electronic circuits atom by atom with tailor-made properties, however, would require the detailed knowledge of the relation between the physical and chemical properties of the respective atoms and their conduction properties, a problem which has been addressed by different methods during the last years [4, 5, 6]. The most simple system for all investigations - including the present - is a one-atom contact between two metallic banks of the same element.

Electrical transport through such contacts is suitably described by the Landauer formalism, which treats it as a wave scattering problem.

The transport properties of the contact connected to the leads are described by a set of transmission coefficients $\{T_n\}$ with $T_n \leq 1$. *E.g.* the conductance $G$ of a contact is $G = G_0 \sum_n T_n$. Here, $G_0 = 2e^2/h$ is the conductance quantum [7]. Since in few-atom metallic point contacts the structure size is of the same order as the Fermi wavelength, such a contact has only a small number $N$ of channels. If the set $\{T_n\}$ is known, all further transport properties, as *e.g.* shot noise, thermopower or superconducting properties of the contact can be deduced.

In order to test basic concepts of the quantum mechanical transport theory, it is of particular interest to study metallic systems transmitting only one single channel with adjustable transmission coefficient. According to a quantum chemical model by Cuevas, Levy Yeyati and Martín-Rodero (CLM) [8, 9] the transmission coefficients of single-atom contacts are a function of the chemical properties of the metal and the atomic arrangement of the region around the central atom. Within their model only single atom contacts of monovalent metals as *e.g.* the alkali or noble metals should transmit one single channel. In particular for Au it has been predicted that the transmission coefficient of this single channel can achieve, in a perfectly ordered geometry of the central atom and its neighbors, a nearly saturated value of $T > 0.99$ [9]. We present here preliminary results of an experiment which allows to determine the transmission coefficients of this model substance.

## 2. DETERMINATION OF THE TRANSMISSION COEFFICIENTS

It has been shown [10] that the set $\{T_n\}$ of atomic-size constrictions is amenable to measurement using the strong non-linearities in the current-voltage ($IV$) characteristics of *superconducting* atomic contacts due to multiple Andreev reflections (MAR). The upper left inset of Fig. 2.1 shows the numerical predictions for a single channel with transmission $T$ [11]-[14]. The $i(V,T)$ curves present a series of sharp current steps at voltage values $eV = 2\Delta/m$, where $m$ is a positive integer and $\Delta$ is the superconducting gap. The order $m = 2, 3, ...$, of a step corresponds to the number of electronic charges transferred in the underlying MAR process. Energy conservation imposes a threshold $eV \geq 2\Delta/m$ for the process of order $m$. For low transmission, the contribution to the current arising from the process of order $m$ scales as $T^m$. The analysis is performed by decomposing the experimental $IV$s through a contact into contributions of $N$ independent terms with the $\{T_n\}$ (where $n = 1, ..., N$) as fitting parameters: $I(V) = \sum_{n=1}^{N} i(V, T_n)$.

Since Au is not superconducting, the described method of determining conduction channels is not directly applicable. However, due to the so-called proximity effect [15, 16], a finite piece of a non-superconducting metal in good contact with a superconducting metal adopts certain superconducting properties, *e.g.* it develops a "minigap" $E_g$ in the quasi-particle excitation spectrum. As will be explained below, the appearance of the minigap is the basic property for determining the channel ensemble. A detailed analysis of the proximity effect in our mesoscopic samples is subject of a separate paper [17].

## 3. EXPERIMENTAL TECHNIQUES

Experimentally stable atomic-size contacts can be achieved with different techniques including STM [18, 19] and mechanically controllable breakjunctions (MCB) [20]. Using such methods it has been shown that smallest stable contacts of gold have most often a conductance close to $G_0$. We have produced a micro-fabricated breakjunction [21] of Al, where the center part of the constriction consists of Au. Using shadow evaporation through a suspended mask we evaporate perpendicular to the substrate surface two Al electrodes separated by a gap of width $w$ with a thickness 300 nm. Without breaking the vacuum, two Au layers of thickness 10 nm are evaporated at two different angles $\pm$ 10° in order to fill the gap and to form a continuous film (see right inset of Fig. 2.1). After lifting off the mask the sample is dry etched to form a free-standing nanobridge. The bridge is broken at the constriction at very low temperatures and under cryogenic vacuum conditions by controlled bending of the elastic substrate mounted on a three-point bending mechanism. Details of the sample preparation and measuring setup are given in [10, 17, 22]. As found in previous experiments [20] the conductance $G$ decreases in steps of the order of $G_0$, with smaller steps within a plateau (see Ref. [10, 23]).

Figure 2.1 shows typical $IV$s of an Al-Au-Al sample (circles) and an Al sample [24] (triangles) obtained at 50 mK for comparable conductances of about 0.7 $G_0$, determined by the slope of the $IV$ at large voltages $V > 0.8$ mV. Both $IV$s exhibit the characteristic features of MAR and a supercurrent. However, the voltage values of the MAR steps are different for both samples. By analyzing $IV$s obtained in the tunnel regime (not shown) [10, 17] we deduce $\Delta/e = 185$ $\mu$V for the Al sample and $E_g/e = 160$ $\mu$V for the Al-Au-Al sample. Because of the small length and layer thickness of the normal metal of this particular Al-Au-Al sample its superconducting properties can be well described by the theory of MAR for BCS superconductors (the gap parameter is then the experimentally determined minigap $E_g$). The $IV$ of the Al-Au-Al sample can

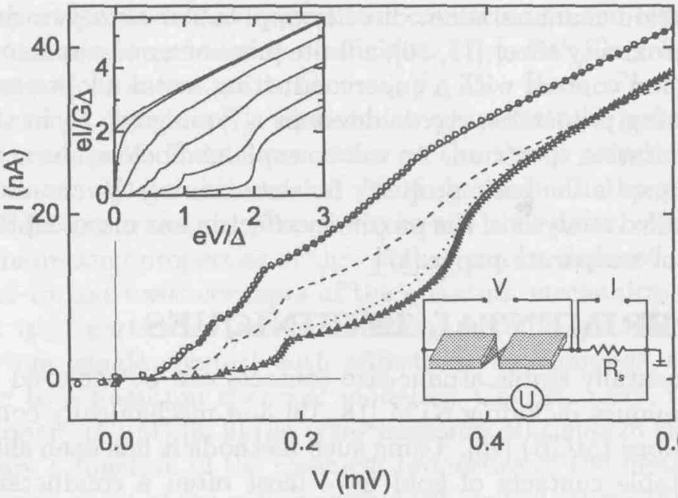


*Figure 2.1* Measured $IV$s for few-atom contacts obtained with the Al-Au-Al sample (circles) and the Al sample (triangles) and best numerical fits (lines). The $\{T_n\}$ and total transmissions $D$ obtained from the fits are: $T = D$=0.692, $E_g/e = 160\ \mu$V for the Al-Au-Al sample and $\{0.387, 0.246, 0.126\}$, $D$=0.759 $\Delta/e = 185\ \mu$V for the Al sample. The dashed (dotted) line is the best fit to the $IV$ of the Al sample assuming one (two) channel(s). Not all measured data points are shown. Left inset: Theoretical $IV$s for a single channel superconducting contact for different values of $T$ (from bottom to top: 0.1, 0.4, 0.7, 0.9, 0.99, 1) after [13]. Both axes are in reduced units. Right inset: Simplified sample geometry of the Al-Au-Al sample and measuring circuit. Dark grey regions: Au, light grey regions: Al.

be described by one single channel without any adjustable parameter, since the transmission of this channel is determined by the slope of the $IV$ at high voltages $eV \gg 2\Delta$ (see line in Fig. 2.1), as predicted by CLM. According to their model, imperfect coupling of the constriction atom to its neighbors reduces the value of $T$ [8, 9]. When pulling the two parts of the bridge apart, it is reasonable to assume that the local order in the central region is changed, explaining the fact that often the last plateau is not flat and its conductance is below $G_0$.

Although the conductance of the Al sample is also below $G_0$, three channels have to be taken into account (solid line). Best fits with one (dashed) or two (dotted) channels reveal systematic deviations from the measured $IV$. If the fitting procedure is performed with more than three channels, the quality of the fit is not improved any more and the transmissions of the supplementary channels turn out to be negligibly small ($< 1$ % of $G$).

Thus, we find for Au stable contacts, whose transport properties can be explained by taking into account only one conduction channel.

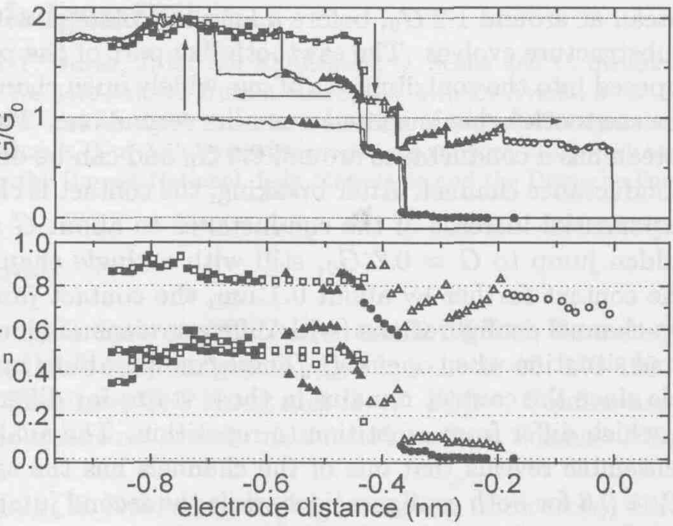


*Figure 2.2* Upper panel: Conductance as a function of electrode distance of an Al-Au-Al sample (with $E_g$=125 $\mu$V) when repeatedly opened and closed. The distance axis has been scaled by the exponential dependence of $G$ in the tunnel regime. Due to hysteresis in the mechanical setup, an varying offset of about 0.03 nm has been subtracted such that the origin of the distance axis is for all repetitions at the position where the contact breaks. Lines: continuous motion at $v \approx$ 10-20 pm/s and dc-conductance measurement with applied magnetic field of 10 mT for suppressing the superconductivity, symbols: sums of the transmission values when motion was stopped for recording $IV$s and determining the channel ensemble: Open symbols: opening, closed symbols: closing; circles (triangles, squares): one (two,three) channels. Not all data are shown. Lower panel: Transmission ensemble.

When further closing the contact to higher conductances, a decomposition analysis as for the Al sample taking into account more channels has to be performed. When the closing is stopped at conductances around 2 $G_0$, stable reproducible configurations can be achieved, which allow for repeated breaking and closing of the contact with the same conduction properties. As an example we plot in Fig. 2.2, a representative subset of conductance *vs.* distance curves of an Al-Au-Al sample, measured below 100 mK during two days when changing the configurations. The data shown as solid lines have been measured when continuously opening at a speed of 10-20 pm/s. For determining the channel ensemble (see lower panel of Fig. 2.2) two opening and closing cycles have been performed with stopping the motion at different positions and recording $IV$ characteristics. Starting at $G \approx 2\ G_0$ from a three channel configuration with one well transmitted channel $T_1 \approx 0.8$ and two almost degenerate ones $T_2 \approx T_3 \approx 0.5$, the conductance jumps down to a short and tilted plateau at around 1.2 $G_0$, before a long last plateau with a reproducible substructure evolves. The sawtooth-like part of the plateau can be decomposed into the contributions of one widely open channel (which reveals the sawtooth behaviour) and a smaller second one. The last part of the plateau has a conductance around 0.8 $G_0$ and can be described by a single conductance channel. After breaking, the contact is closed by an almost exponential increase of the conductance to about $G \approx 0.07\ G_0$ and a sudden jump to $G \approx 0.7\ G_0$, still with a single channel. After closing the contact further by about 0.1 nm, the contact jumps to one of two two-channel configurations (with different transmissions than the two-channel situation when opening). These configurations appear to be metastable since the contact remains in those states for different length intervals, which differ from repetition to repetition. The analysis of the channel ensemble reveals that one of the channels has the same transmission $T_1 \approx 0.6$ for both configurations while the second jumps between two very different values (0.3 and 0.8). A possible interpretation of this behaviour would be one atom in a stable position and a second one alternating between two almost degenerate positions.

Finally the contact arrives at its initial stable plateau with three channels. The transmission values as well as the substructure of the plateau are reproducible within the accuracy of the conductance measurement in the continuous measurements and the determination of the channels ($\approx 3\%$). Although not all details of the substructure are observed in any of the $\approx 20$ repetitions, the substructure of this stable plateau is used to distinguish the extrinsic hysteresis of the mechanical setup and the intrinsic hysteresis of the atomic motion. From the distance values we have subtracted varying offsets of the order of 0.1 nm such that the contacts break at zero. The mechanical hysteresis has been determined such that the curvatures of the stable three-channel plateaux when opening and closing the contact overlay. The remaining hysteresis of $\approx 0.4$ nm is of the order of the lattice spacing of gold and is thus an intrinsic effect of the atomic contact [25]. The reproducible situation was kept until the contact was closed thoroughly. These observations support the assumption that the conductance of the whole system is determined by the central atom and its coupling to the nearest neighbors.

In conclusion, we have presented an investigation of the transport properties of gold tunnel and few-atom contacts with superconducting leads. We have analyzed quantitatively the *IV* characteristics of few-atom contacts containing up to three conduction channels. Single-atom gold contacts accommodate one conduction channel in accordance with theoretical predictions.

## Acknowledgements

We thank Y. Naveh, J. M. van Ruitenbeek, G. Schön and C. Strunk for helpful discussions. We have enjoyed fruitful interaction with D. Averin, J. C. Cuevas and A. Levy Yeyati, and we thank them for providing us with their respective computer codes. E. S. thanks H. v. Löhneysen for continuous support. This work was partially supported by the Bureau National de la Métrologie and the Deutsche Forschungsgemeinschaft.

## References

[1] G. Binnig, H. Rohrer, Ch. Gerber and E. Weibel, Tunneling through a controllable vacuum gap, Appl. Phys. Lett. **40**, 178-180 (1982).

[2] M. F. Crommie, C. P. Lutz and D. M. Eigler, Confinement of electrons to quantum corrals on a metal surface, Science **262**, 218-220 (1993).

[3] G. Binnig, H. Rohrer, Scanning tunneling microscopy, IBM J. Res. Dev. **30**, 355 (1986).

[4] N. D. Lang, Resistance of atomic wires, Phys. Rev. B **52**, 5335-5342 (1995).

[5] C. C. Wan, J.-L. Mozos, G. Taraschi, J. Wang and H. Guo, Quantum transport through atomic wires, Appl. Phys. Lett. **71**, 419-421 (1997).

[6] A. Yazdani, D. M. Eigler and N. D. Lang, Off-resonance conductance through atomic wires, Science **272**, 1921-1924 (1996).

[7] R. Landauer, Electrical resistance of disordered one-dimensional lattices. Philos. M. **21**, 863-867 (1970).

[8] J. C. Cuevas, A. Levy Yeyati and A. Martín-Rodero, Microscopic origin of the conducting channels in metallic atomic-size contacts, Phys. Rev. Lett. **80**, 1066-1069 (1998).

[9] A. Levy Yeyati, A. Martín-Rodero and F. Flores, Conductance quantization and electron resonances in sharp tips and atomic size contacts, Phys. Rev. B **56**, 10369-10372 (1997).

[10] E. Scheer, P. Joyez, D. Esteve, C. Urbina and M. H. Devoret, Conduction channel transmission of atomic-size aluminum contacts, Phys. Rev. Lett. **78**, 3535-3538 (1997).

[11] G. B. Arnold, Tunneling without the tunneling Hamiltonian II. Subgap harmonic structure, Journal of Low Temp. Phys. **68**, 1-27 (1987).

[12] D. Averin and A. Bardas, AC Josephson effect in a single quantum channel, Phys. Rev. Lett. **75**, 1831-1834 (1995).

[13] J. C. Cuevas, A. Martín-Rodero and A. Levy Yeyati, Hamiltonian approach to the transport properties of superconducting quantum point contacts, Phys. Rev. B **54**, 7366-7379 (1996).

[14] E. N. Bratus, V. S. Shumeiko, E. V. Bezuglyi and G. Wendin, dc-current transport and ac Josephson effect in quantum junctions at low voltage, Phys. Rev. B **55**, 12666-12677 (1997).

[15] D. Esteve, The proximity effect in mesoscopic diffusive conductors. In *Mesoscopic Electron Transport* (eds. L. L. Sohn, L. P. Kouwenhoven and G. Schön, Kluwer Academic Publishers, 1997) pp. 375-406, and references therein.

[16] W. Belzig, F. K. Wilhelm, C. Bruder, G. Schön and A. D. Zaikin, Quasiclassical Greens function approach to mesoscopic superconductivity, Superlattices and Microstructures **25**, 1251-1288 (1999).

[17] E. Scheer, W. Belzig, Y. Naveh, D. Esteve, M. H. Devoret and C. Urbina, Proximity effect and multiple Andreev reflections in gold atomic contacts, submitted for publication.

[18] L. Olesen, E. Lægsgaard, I. Stensgaard, F. Besenbacher, J. Schiøtz, P. Stoltze, K. W. Jacobsen and J. K. Nørskov, Quantized conductance in an atom-sized point contact, Phys. Rev. Lett. **72**, 2251-2254 (1994).

[19] N. Agraït, J. G. Rodrigo and S. Vieira, Conductance steps and quantization in atomic-size contacts, Phys. Rev. B **47**, 12345-12348 (1996).

[20] J. M. van Ruitenbeek, Quantum point contacts between metals; in *Mesoscopic Electron Transport* (eds. L. L. Sohn, L. P. Kouwenhoven and G. Schön, Kluwer Academic Publishers) pp. 549-579, and references therein.

[21] J. M. van Ruitenbeek, A. Alvarez, I. Piñeyro, C. Grahmann, P. Joyez, M. H. Devoret, D. Esteve and C. Urbina, Adjustable nanofabricated atomic size contacts Rev. Sci. Inst. **67**, 108-111 (1996).

[22] E. Scheer, P. Joyez, D. Esteve, C. Urbina and M. H. Devoret, Conduction channels of superconducting quantum point contacts, to appear in Physica B.

[23] E. Scheer, N. Agraït, J. C. Cuevas, A. Levy Yeyati, B. Ludoph, A. Martín-Rodero, G. Rubio Bollinger, J. M. van Ruitenbeek and C. Urbina, The signature of chemical valence in the conduction through a single-atom contact, Nature **394**, 154-157 (1998).

[24] The Al sample has been fabricated as explained in [10] within a single evaporation step through a mask without the bridge.

[25] C. Untiedt, G. Rubio, S. Vieira and N. Agraït, Fabrication and characterization of metallic nanowires, Phys. Rev. B **56**, 1251-1288 (1997).